# Prediction of novel ultrahard phases in the B–C–N system from first principles: Progress and problems

Vladimir Solozhenko, Samir Matar

# Prediction of novel ultrahard phases in the B–C–N system from first principles: progress and problems

Vladimir L. Solozhenko[1,*] and Samir F. Matar[2]

[1] LSPM–CNRS, Université Sorbonne Paris Nord, 93430 Villetaneuse, France

https://orcid.org/0000-0002-0881-9761

[2] Lebanese German University (LGU), Sahel Alma, Jounieh, Lebanon

https://orcid.org/0000-0001-5419-358X

ABSTRACT

Modern synthesis of superhard and, especially, ultrahard phases is a very fascinating area of research that could lead to design of new industrially important materials. Computational methods built within the well-established quantum mechanics framework of the density functional theory (DFT) play an important role in search for these advanced materials and prediction of their properties. The close relationship between the physical properties of carbon and boron nitride has led to particular interest in the B-C-N ternary system, characterized by small radii of the elements, resulting in short interatomic distances and reduced volumes – the parameters being 'recipes' for very high hardness in three dimensional structures. The purpose of this review is to provide a brief outline of recent developments and problems in predicting novel ultrahard carbon allotropes as well as binary and ternary compounds of the B-C-N system with particular emphasis on the analysis of the models used to evaluate hardness of theoretically predicted structures.

Keywords: B-C-N system; DFT; crystal structure, elastic moduli; hardness.

* Corresponding author (vladimir.solozhenko@univ-paris13.fr)

## Introduction

Historically, research in the field of ultrahard materials (usually defined as having Vickers hardness $H_V \geq 80$ GPa) was initiated a century ago, triggered by increasing industrial application of diamond, the hardest ($H_V$ up to 120 GPa) known material. However, use of diamond in mining and tooling raised problems due to high cost of natural diamonds, on the one hand, and its relatively low stability at even moderate operating temperatures, on the other hand. The first problem was solved by the development of high-pressure synthesis of diamond [1], but its high reactivity with oxygen and ferrous metals remained a problem that required further efforts to find reliable substitutes for diamond.

An interim solution was the synthesis of cubic boron nitride (cBN) [2], which is half as hard as diamond, but has much higher thermal and chemical stability. It should be noted that in terms of electronic structure BN is equivalent to 2C (*vide infra*). The close relationship between the physical properties of carbon allotropes and BN polymorphs has facilitated search for ultrahard phases in the B–C–N ternary system constituted by light elements with small radii, resulting in short interatomic distances and reduced volumes – all the parameters being 'recipes' for high strength and hardness.

Until very recently diamond was the only known material which is ultrahard. However, in 2001, cubic $BC_2N$, a ternary compound that is halfway between diamond and BN in composition was synthesized [3]. Vickers hardness of 76(4) GPa [4] makes it the second member of the ultrahard phases family. In 2009, the third ultrahard phase, diamond-like $BC_5$, was discovered [5] which possesses Vickers hardness of 71(8) GPa, unusually high for superhard materials fracture toughness (~10 $MPa \cdot m^{1/2}$), and very high (up to 1900 K) thermal stability. Both novel ultrahard phases have been synthesized at very high pressures and temperatures with *in situ* control using synchrotron X-ray diffraction which indicates that the experimental search for such phases is a challenging task [6].

Since experimental materials discovery is suffering from the high labor costs and limitations inherent to the trial-and-error methods, theoretical approaches for predicting mechanical properties of solids have been developed, from empirical models of hardness [7-10] to *ab initio* calculation of elastic constants [11,12] and computational discovery of superhard materials [13-15]. Thus, the modern algorithms and powerful computers can be used to search for materials with exceptional mechanical properties.

Studies within the B-C-N ternary system are a growing area of exploration, complementing the competence of experimenters using modern low- and high-pressure techniques, well adapted to light elements with high purity sources and theorists employing structure research tools such as CALYPSO [16] and USPEX [17,18] to access accurate characterizations of electronic structures and energy related quantities such as mechanical and dynamic signatures from quantum mechanics software built in the framework of the density functional theory (DFT) (cf. Annex). Calculation results serve as both interpretive and predictive tools for new materials with desired properties.

Since the present paper is not intended to be a comprehensive and exhaustive review, we aim to focus on presentation of the recent developments and problems in this emerging research field, and illustrate

the subject using examples from our own studies (both published and unpublished) (Fig. 1). To highlight the structural and physical properties in the main body of review, we present the computational framework in the Annex.

## I. Elements

Carbon and boron (in particular, their dense allotropes, i.e. diamond and γ-$B_{12}$ [19]) are the hardest elements. We shall not discuss boron here (the problem of searching for its superhard forms was already addressed in the recent review [20]), but will rather concentrate on carbon. The main research efforts with respect to carbon are focused on the search for new dense allotropes with mechanical properties close to those of diamond. Diamond is known to exist in two forms: the cubic one that belongs to space group *Fm*-3*m* (No. 227), and rare hexagonal form called 'lonsdaleite' (space group $P6_3/mmc$, No. 194). Recently, however, the existence of lonsdaleite as a discrete phase has been questioned, and it has been interpreted as a cubic diamond dominated by extensive twins and stacking faults [21].

It should be noted that information on 3-periodic carbon allotropes extracted from scientific literature is gathered and indexed in the "SACADA" database [22]. Currently, it counts 524 unique carbon allotropes. From the structural point of view, and using chemistry terms, diamond is characterized by tetrahedral ($sp^3$) carbon, as in the methane gas molecule $CH_4$, and its crystal structure demonstrates three-dimensional stacking of corner sharing *C4* tetrahedra. In contrast, graphite is characterized by a layered structure where carbon is $sp^2$ hybridized, as in the ethene gas molecule $C_2H_4$. While diamond is a large band gap insulator with $E_{gap} \approx 5$ eV, graphite is a semiconductor with a very small gap. Mixed $sp^2$-$sp^3$ hybridizations carbon was recently reported for a new stable metallic allotrope *hex*-$C_{18}$ (called 18*H* carbon) which belongs to space group *P6*/*mmm* (No. 191) [23].

Carbon in linear triatomic C–C–C arrangement is found in carbon suboxide $C_3O_2$ where carbon is $sp^2$ hybridized. In solid state the linear configuration is kept for carbon suboxide which is a molecular solid where weak (van der Waals-like) interactions prevail between separate molecules. Rarely occurring tricarbon $C_3$ molecule was observed in interstellar space, mainly in tails of the comets (e.g. Hale-Bopp, C/1995O1), and experimentally identified by spectroscopic measurements [24]. Recently [25], we considered linear C–C–C in two novel structures: (i) *rh*-$C_3$ (or *hex*-$C_9$) (space group *R*-3*m*, No. 166) based on rhombohedral sodium azide characterized by the presence of linear $N_3$ fragment (Fig. 2a), and (ii) *hex*-$C_6$ (space group $P6_3/mmc$, No. 194) derived from lonsdaleite through the insertion of one extra carbon atom along the *c*-axis at 2d (2/3,1/3,¼) Wyckoff position (Fig. 2b). From geometry optimization to energy ground state within DFT (cf. Annex), energies and the energy-derived quantities were found within range of diamond and lonsdaleite.

The elastic properties of 'tricarbon' allotropes *rh*-$C_3$ and *hex*-$C_6$ were determined by performing finite distortions of their lattices. The elastic constants $C_{ij}$ were derived from the strain - stress relationship. Indexes i and j represent directions: when i = j, the elastic constants correspond to application of

unidirectional stress (as in the case of $C_{33}$ elastic constant discussed below), and when $i \neq j$, the elastic constants are relevant to applying shear stress. For both allotropes all calculated $C_{ij}$ values are positive, and their combinations obey the rules pertaining to mechanical stability of the phases. The bulk ($B_V$) and shear ($G_V$) moduli were calculated from elastic constants following the Voigt method [26] based on a uniform strain.

Vickers hardness of new carbon allotropes was predicted using four modern theoretical models [8,19,27,28]. The thermodynamic model [27] is based on thermodynamic properties and crystal structure, empirical Chen-Niu [8] and Mazhnik-Oganov [10] models use the elastic properties, and Lyakhov-Oganov approach [28] considers topology of the crystal structure, strength of covalent bonding, degree of ionicity and directionality. The fracture toughness ($K_{Ic}$) was evaluated within the Mazhnik-Oganov model [10]. Tables 1,2 present the hardness values calculated using all four models, and other mechanical properties such as bulk ($B$), shear ($G$) and Young's ($E$) moduli, the Poisson's ratio ($\nu$) and fracture toughness ($K_{Ic}$).

As it has been reported earlier [29], in the case of ultrahard compounds of light elements the thermodynamic model shows surprising agreement with available experimental data. Moreover, its use is preferable in the case of hybrid dense carbon allotropes, for which Lyakhov-Oganov model gives underestimated hardness values whereas the empirical models are not reliable. For this reason, both new 'tricarbon' allotropes should be considered as ultrahard phases.

Although hardness and elastic moduli of *rh*-$C_3$ and *hex*-$C_6$ are somewhat lower than those of diamond, a strong anisotropy was found for both 'tricarbon' allotropes with exceptionally large $C_{33}$ values along the hexagonal *c*-axis, i.e. $C_{33} = 1636$ GPa for *rh*-$C_3$ (Fig. 2a) and $C_{33} = 1610$ GPa for *hex*-$C_6$, exceeding the corresponding value for lonsdaleite, $C_{33} = 1380$ GPa. Vickers hardness predicted using four theoretical models (Tables 1,2) points out to a slightly lower $H_V$ values for these new carbon allotropes compared to diamond (both cubic and hexagonal), but much higher than hardness of the vast majority of recently predicted carbon allotropes such as $C_{14}$, $C_{16}$, $C_{24}$, $C_{36}$, etc. [30-33]. Thus, both *rh*-$C_3$ and *hex*-$C_6$ have exceptional mechanical properties and can be considered as prospective ultrahard phases [34].

Dynamic stability of 'tricarbon' allotropes was confirmed by the phonons calculations. All frequencies are positive, with the particular feature of a gap in the highest frequency optical phonons domain, not observed in lonsdaleite, and caused by the rigidly aligned $C_3$ unit. A remarkable consequence of the presence of two carbon hybridizations ($sp^1$ and $sp^3$) is the occurrence of a metallic character in the electronic band structure of both 'tricarbon' allotropes, similar to that previously observed for hexagonal $C_{18}$ [23] and monoclinic $C_{12}$ [35] characterized by mixed $sp^2$-$sp^3$ and $sp^1$-$sp^2$ hybridizations, respectively.

Another novel ultrahard carbon allotrope, body-centered tetragonal $C_6$ (space group *I*-4*m*2, No. 119) presenting mixed $sp^2/sp^3$ hybridizations has been proposed very recently by crystal chemistry approach and studied for the ground state structure and stability using DFT calculations [36]. Since *C4*

tetrahedra are in-plane stacked with corner-sharing and connected out-of-plane with C–C trigonal carbon (Fig. 2c), a close relationship with so-called 'glitter', a hypothetical dense carbon network invented in 1994 [37], is apparent, and thus the new allotrope was named 'neoglitter'. Besides the mechanical stability (positive values of elastic constants and their combinations), 'neoglitter' is also dynamically stable as it follows from its phonon band structure. Novel allotrope reveals exceptional mechanical properties i.e. very high hardness and elastic moduli (see Tables 1,2) being conductive due to the metallic-like electronic structure which is mainly caused by the itinerant role of trigonal carbon $\pi$-electrons.

Since Vickers hardness calculated in the framework of thermodynamic model exceeds 80 GPa for three novel carbon allotropes described above, they all should be attributed to the family of ultrahard phases.

## II. Binary compounds

Hardness of dense compounds of the binary B–N system - cubic BN [2], rhombohedral $B_{13}N_2$ [38,39] and tetragonal $B_{50}N_2$ [40] - does not exceed $H_V = 62$ GPa for single-crystal cBN [4], i.e. they all belong to the group of superhard phases. Special mention should be given to nanocrystalline cBN [41] with Vickers hardness up to 85 GPa [42], mainly due to the Hall–Petch effect i.e. nanosize effect which restricts dislocation propagation through the material.

We will focus in more detail on two other binary systems, i.e. C–N and B–C, in which compounds with very high hardness have been predicted.

### Carbon nitrides

The main interest in studying the C–N system is a result of numerous (but unsuccessful) attempts to synthesize hypothetical ultrahard $C_3N_4$. In the 1990s Liu *et al.* [43,44] and Teter & Hemley [45] predicted a number of dense low-compressibility carbon nitrides of $C_3N_4$ stoichiometry that were claimed to exhibit bulk moduli and hardness higher than those of diamond because of the short length and high covalence of the C-N bonds. However, our analysis in the framework of the thermodynamic model of hardness, reveals that Vickers hardness of the densest hypothetical cubic (*P*-43*m* [44] and *I*-43*d* [45]) and pseudocubic (*P*-42*m* [45]) polymorphs of $C_3N_4$ does not exceed 73 GPa.

Besides isoelectronic with diamond carbon nitrides of $C_3N_4$ stoichiometry [46], carbon subnitrides of $C_{11}N_4$ stoichiometry were also studied [47] as they allow modeling of $CN_x$ films with less than 30 at% N which are usually forming when vapor phase deposition techniques are used [48]. In this context structural models of $C_{11}N_4$ phases accounting for the low nitrogen content were derived from diamond being isoelectronic with it, through creating defects. Indeed, diamond expressed as 2C in primitive cell has 8 valence electrons, and $C_{11}N_4$ has $11\times4+4\times5 = 64 = 8\times8$ electrons, i.e. an integer multiple of 8.

In the present paper a novel (ultra)hard tetragonal $C_{11}N_4$ (space group *P*-4*m*2, No. 115) was derived from $C_{16}$, a 2×2×1 cell of body-centered tetragonal $C_4$ diamond-like structure [49] (Fig. 3a). In this template a defect was created at the center of the tetragonal cell by removal of the yellow carbon atom (see Fig. 3a) and replacing the 4 surrounding carbon atoms by nitrogen (blue spheres in Fig. 3b). The resulting fully relaxed carbon subnitride $C_{11}N_4$ was analyzed for the cohesive energy $E_{coh}$ obtained from subtracting the atomic energies of 11 C and 4 N atoms from the calculated total energy. $C_{11}N_4$ was found cohesive with $E_{coh}$ = -1.93 eV/atom which is lower than the corresponding value for pristine $C_{16}$ ($E_{coh}$ = -2.49 eV/atom, the value identifying diamond). This is quite expected, since $C_{11}N_4$ results from the defect diamond-like structure of $C_{16}$. Such observations are also valid for other binary compounds resulting from perturbation of the diamond lattice.

The lattice parameters of $C_{11}N_4$ are $a = b = 4.95258$ Å and $c = 3.52024$ Å with nitrogen atom occupying the 4k site (0.50000, 0.24200, 0.72825) and four inequivalent carbon atoms locating at the 1a (0.00000, 0.00000, 0.00000), 2g (0.50000, 0.00000, 0.97312), 4i (0.25368, 0.25368, 0.50000) and 4j (0.24974, 0.00000, 0.23750) sites. Besides being cohesive, $C_{11}N_4$ was found mechanically stable with the whole set of elastic constants positive, as well as dynamically stable with positive acoustic and optic phonons frequencies.

Calculated values of hardness and elastic moduli of *tet*-$C_{11}N_4$ are listed in Tables 1,2. Although bulk and shear moduli of novel carbon subnitride are lower than the corresponding values for high-density $C_3N_4$, its Vickers hardness $H_V = 76$ GPa is higher than that of all hypothetical high-density polymorphs of $C_3N_4$ [43-45].

The electronic band structure of novel tetragonal $C_{11}N_4$ is shown in Fig. 3c, characterizing an insulator with a gap value slightly below 5 eV, between from Γ (valence band) to Z (conduction band), similar to that of diamond, as a result of both structures being isolectronic as mentioned above.

Boron carbides

Rhombohedral boron carbide $B_4C$ ($B_{12}C_3$) is the most important, well-studied and widely used compound of the B–C binary system, however, its Vickers hardness does not exceed 37 GPa [50]. Synthesis of diamond-like $BC_5$ with hardness above 70 GPa [5] has stimulated interest in the study of carbon-rich compounds of this system. Thus, four polymorphs of $BC_5$ were predicted from first-principles structural optimizations [51], for two of which (tetragonal *I*-4*m*2 and triclinic *P*-1) Vickers hardness of about 80 GPa was claimed. However, our assessments (the results for the densest tetragonal $BC_5$ are presented in Tables 1,2) showed that hardness of all predicted phases was overestimated by ~15% as a result of the use of unreliable empirical correlation between shear modulus and hardness.

A similar situation is observed in the case of five predicted $BC_7$ polymorphs [52]: the claimed hardness values (e.g. 81 GPa for orthorhombic *Pmm*2 and 78 GPa for cubic *P*-43*m* phases) are also overestimated by 10-15% as a result of using the empirical microscopic hardness model (see our

results for cubic $BC_7$ in Tables 1,2), and thus these phases, as well as $BC_5$ polymorphs, cannot be considered ultrahard. However, one may expect that a further decrease in boron content will be accompanied by hardness increase of the forming B-C binary compound(s).

Very recently, the latter has been confirmed by prediction of trigonal $BC_{11}$ (space group $P3m1$, No. 156) [53] produced by the substitution of carbon with boron in the diamond-like *hex*-$C_{12}$ template [54] that led to lowering of the crystal symmetry down to trigonal.

In the context of energy criterion, it was interesting to position the novel carbon-rich $BC_{11}$ among other B-C binary compounds. Comparison of *trig*-$BC_{11}$ cohesive energy with those reported for *trig*-$BC_5$ [51] and *trig*-$BC_7$ [52] shows a clear trend of decreasing $E_{coh/atom}$ with increasing boron content: -2.49 eV (diamond) < -2.33 eV ($BC_{11}$: 8.3 at% B) < -2.24 eV ($BC_7$: 12.5 at% B) < -2.16 eV ($BC_5$: 16.7 at% B). Besides being more cohesive than two other binary compounds, *trig*-$BC_{11}$ was also found to be mechanically (elastic constants) and dynamically (phonon band structures) stable.

Crystal structures of template *hex*-$C_{12}$ and *trig*-$BC_{11}$ are shown in Fig. 4. In *hex*-$C_{12}$ the carbon network is perfectly covalent in all dimensions. Changes are observed for *trig*-$BC_{11}$ featuring large covalent part where the carbon networks remain like *hex*-$C_{12}$, but not in the surrounding of boron atoms whose charge density is transferred to carbon due to the larger electronegativity of carbon. Regarding its electronic band structure, bands belonging to boron states were found crossing the Fermi level $E_F$ signaling a metallic character arising from one electron-less B ($2s^2,2p^1$) versus C ($2s^2,2p^2$) in wide gap insulating diamond.

Hardness of *trig*-$BC_{11}$ calculated using four models, as well and other mechanical properties, are given in Tables 1,2. Although the introduction of boron atoms into the diamond crystal lattice is predictably lowering the hardness, it remains high enough (> 80 GPa) to consider *trig*-$BC_{11}$ as ultrahard phase, in contrast to other reported binary compounds of the B–C system [51,52,55].

## III. Ternary compounds

Interest in search for possible 'hybrid' structures of carbon and boron nitride and prediction of their properties (mechanical, in particular) has especially grown after the synthesis of ultrahard cubic $BC_2N$ [3]. Over the past 20 years, several dozen papers have been published on the subject, but here we will focus only on those that claimed the 'ultrahardness' ($H_V \geq 75$ GPa) of the predicted phases. In addition to different $BC_2N$ structures [29,56-58], ultrahard phases of BCN [59], $BC_4N$ [60-62], $BC_6N$ [63,64] and $BC_{10}N$ [65] compositions have been reported.

Our assessments for orthorhombic ($P222_1$) and trigonal ($P3m1$) $BC_2N$ [56] as well as for novel rhombohedral ($R3m$) $BC_2N$ [29] (Fig. 5a) show that they all have Vickers hardness of the order of 75 GPa (see Tables 1,2; the $H_V$ values calculated using the thermodynamic model are the most reliable), i.e. almost the same as experimental value 76(4) GPa for cubic $BC_2N$ [3,4]. As for 79.7 GPa

hardness claimed for calculated low-energy zinc-blende $BC_2N$ [58], it seems to be overestimated due to the use of the empirical hardness model suggested by Gao *et al*. [66] (see Table 3).

The similar situation is observed for trigonal (*P*3*m*1) [60] and orthorhombic (*Imm*2) [61] $BC_4N$, and tetragonal (*P*−42*m*) [63], rhombohedral (*R*3*m*) [63] and monoclinic (*Pm* and *Cm*) [64] $BC_6N$. In all these cases, the use of Gao's model results in a 4-11% hardness overestimation compared to the values we obtained in the framework of the thermodynamic model of hardness (see Table 3).

Use of another empirical so-called 'microscopic' model of hardness suggested by Tian *et al*. [9] for trigonal $BC_4N$ [62] and $BC_{10}N$ [65] leads to even higher (15-20%) overestimations of hardness compared to the thermodynamic model (see Table 3).

In general, according to our estimates, the hardness of dense ternary phases of the aforementioned compositions varies in the 72-76 GPa range, i.e. they all can be considered as (ultra)hard. Regarding possible equiatomic (B:C:N = 1:1:1) phases, their hardness should be even lower (~70 GPa); see, e.g. $H_V$ values for trigonal (*P*-3*m*1) and tetragonal ($I4_1md$) BCN [59] (Table 3).

The electronic band structure of rhombohedral $BC_2N$ [29] (Fig. 5c) is characteristic of an insulator, alike diamond. In fact, they both have valence electron count multiple of 8 ($C_2$) i.e., 16 (2×8) for $BC_2N$ and 32 (4×8) for diamond ($C_8$).

Below we discuss in more detail tetragonal ($P4_2mc$) equiatomic boron carbonitride (Fig. 5b) recently proposed by us using crystal chemistry rationale and DFT calculations [67].

Compounds containing $CN^-$ anion (such as ionic sodium cyanide $Na^{1+}CN^{1-}$) are called 'cyanides'. Since boron is metalloid (i.e. half-way between metal and non-metal), its combination with nitrogen leads to the equiatomic boron nitride BN that could be expressed as '$B^{3+}N^{3-}$' considering its ionic-like nature. However, BN is rather a polar covalent compound as it can be inferred from the Pauling electronegativity difference ($\Delta\chi$). Considering the average electronegativity of CN: $\langle\chi(CN)\rangle = (2.55+3.44)/2 \sim |3.0|$, NaCN has $\Delta\chi = 0.9–3.0 = |2.1|$, whereas BN is characterized by $\Delta\chi = 2.04–3.44 = |1.4|$. For presently proposed BCN $\Delta\chi = 2.04–3.0 = |0.96|$ which indicates a decrease of ionic character in the NaCN → BN → BCN row.

In the framework of crystal chemistry approach we considered three template structures for BCN: octahedral (CoCN), square-planar (NaCN) and linear (CuCN). The square-planar *BC2N2* coordination was found the most stable among all three templates in terms of cohesive energy, but despite the relative stability it remains a non-compact 2D-like structure. Therefore, as 3D template allowing tetrahedral coordination for B with C and N, and connected *BC2N2* tetrahedra we used tetragonal hexacarbon $C_6$, so-called 'glitter' [37] which possesses two types of carbon: tetrahedral C1 and trigonal C2, the latter forming C2-C2 pairs that separate the $C1C2_4$ tetrahedra. The structure shown in Fig. 6a featuring the charge density projections reveals the two types of carbons in 'glitter' structure, and the corresponding $C1C2_4$ tetrahedra (C1: $sp^3$-like carbon). With appropriate substitutions of carbon for boron and nitrogen leading to BCN, the ground state energy configuration of derived 3D structure was found to be more cohesive than the 2D-like candidate mentioned above.

The resulting BCN ($B_2C_2N_2$) structure sketched in Fig. 6b shows $BC_2N_2$ tetrahedra replacing $C1C2_4$ tetrahedra in 'glitter' $C_6$, and large differences in charge density distribution as compared to $C_6$ with charge density concentration skewed toward C–N bond, and larger intensity on N versus C. Such $B \rightarrow C \rightarrow N$ charge transfers are expected from the Pauling electronegativities: $\chi(B) = 2.04 < \chi(C) = 2.55 < \chi(N) = 3.44$. In the case of BN, 3 electrons depart from B to N leading to $B^{3+}N^{3-}$. In BCN we equally observe $B^{3+}$, but the negative '3-' charge is now distributed between C and N with larger value on N due to its larger electronegativity *versus* C, and one gets $B^{3+}C^{0.316-}N^{2.684-}$. As it follows from our results, cohesive tetragonal BCN is mechanically (elastic constants) and dynamically (phonons) stable. An interesting feature of this phase is that at a relatively low density (2.783 g/cm$^3$) it is characterized by a very high hardness $H_V$ = 65 GPa (i.e. harder than single-crystal cubic boron nitride with density of 3.486 g/cm$^3$ [68]), highly likely due to presence of both tetrahedral ($sp^3$) and trigonal ($sp^2$) carbons in its crystal structure. Such mixed hybridizations in tetragonal BCN leads to its weakly metallic behavior as illustrated by the electronic band structure in Fig. 5d exhibiting a few bands crossing the Fermi level $E_F$.

## IV. Conclusions

Modern high-pressure synthesis of superhard and, especially, ultrahard phases is a very fascinating area of research that could lead to the production of industrially important new materials. However, this field is still in its infancy, and a large number of new super- and ultrahard phases still remains to be discovered. Theoretical predictions play an important role in the present search for advanced materials with desired properties (mechanical, in particular). In this review we have illustrated with selected examples the wealth of (ultra)hard allotropes and phases in the B–C–N ternary system, theoretical (crystal chemistry considerations combined with quantum mechanics calculations) study of which is very active area of research.

At the same time, precise calculations of mechanical properties of superhard materials (hardness, in particular) often lie beyond the capabilities of the most advanced and modern techniques. Thus, we should state that neither widely used empirical models [7-10,66] nor machine learning [14,65,69] allow us to reliably estimate hardness of newly predicted superhard and, especially, ultrahard phases. The only model that seems to work in these cases is the thermodynamic model [27]. Besides, not all theoretically predicted structures exist or can be synthesized. A vivid illustration is the case of hypothetical cubic $C_3N_4$ with a bulk modulus claimed to be higher than that of diamond [45]. Despite the enormous efforts (new attempts are still being undertaken), this phase has not been synthesized so far, and its expected ultrahardness has never been demonstrated.

Finally, it should be noted that the search for new ultrahard phases is indeed at the frontier of fundamental science, and promises great prospects for the creation of new materials that are needed for existing and prospective applications. However, the recent advances in this field clearly show that phases with hardness exceeding that of diamond are highly unlikely, or even impossible [70].

## References


[1] F.P. Bundy, H.T. Hall, H.M. Strong, R.H. Wentorf, Man-made diamonds. *Nature* **176** (1955) 51-55.

[2] R.H. Wentorf, Cubic form of boron nitride. *J. Chem. Phys.* **26** (1957) 956.

[3] V.L. Solozhenko, D. Andrault, G. Fiquet, M. Mezouar, D.C. Rubie, Synthesis of superhard cubic $BC_2N$. *Appl. Phys. Lett.* **78** (2001) 1385-1387.

[4] V.L. Solozhenko, S.N. Dub, N.V. Novikov, Mechanical properties of cubic $BC_2N$, a new superhard phase. *Diam. Relat. Mater.* **10** (2001) 2228-2231.

[5] V.L. Solozhenko, O.O. Kurakevych, D. Andrault Y. Le Godec, M. Mezouar, Ultimate metastable solubility of boron in diamond: Synthesis of superhard diamondlike $BC_5$. *Phys. Rev. Lett.* **102** (2009) 015506.

[6] Y. Le Godec, A. Courac, V.L. Solozhenko, High-pressure synthesis of superhard and ultrahard materials. *J. Appl. Phys.* **126** (2019) 151102.

[7] F. Gao, Theoretical model of intrinsic hardness. *Phys Rev. B* **73** (2006) 132104.

[8] X.Q. Chen, H. Niu, D. Li, Y. Li, Modeling hardness of polycrystalline materials and bulk metallic glasses. *Intermetallics* **19** (2011) 1275-1281.

[9] Y. Tian, B. Xu, Z. Zhao, Microscopic theory of hardness and design of novel superhard crystals. *Int. J. Refract. Met. Hard Mater.* **33** (2012) 93-106.

[10] E. Mazhnik, A.R. Oganov, A model of hardness and fracture toughness of solids. *J. Appl. Phys.* **126** (2019)125109.

[11] H. Yao, L. Ouyang, W.-Y. Ching, Ab initio calculation of elastic constants of ceramic crystals. *J. Am. Ceram. Soc.* **90** (2007) 3194-3204.

[12] W.F. Perger, J. Criswell, B. Civalleri, R. Dovesi, Ab-initio calculation of elastic constants of crystalline systems with the CRYSTAL code. *Comput. Phys. Commun.* **180** (2009) 1753-1759.

[13] A.G. Kvashnin, Z. Allahyari, A.R. Oganov, Computational discovery of hard and superhard materials. *J. Appl. Phys.* **126** (2019) 040901.

[14] P. Avery, X. Wang, C. Oses, E. Gossett, D.M. Proserpio, C. Toher, S. Curtarolo, E. Zurek, Predicting superhard materials via a machine learning informed evolutionary structure search. *npj Comput. Mater.* **5** (2019) 89.

[15] Z. Allahyari, A.R. Oganov, Coevolutionary search for optimal materials in the space of all possible compounds. *npj Comput. Mater.* **6** (2020) 55.

[16] S. Zhang, J. He, Z. Zhao, D. Yu, Y. Tian, Discovery of superhard materials via CALYPSO methodology. *Chin. Phys. B* **28** (2019)106104.

[17] A.R. Oganov, C.W. Glass, Crystal structure prediction using ab initio evolutionary techniques: Principles and applications. *J. Chem. Phys.* **124** (2006) 244704.

[18] C.W. Glass, A.R. Oganov, N. Hansen, USPEX – Evolutionary crystal structure prediction. *Comput. Phys. Commun.* **175** (2006) 713-720.

[19] A.R. Oganov, J. Chen, C. Gatti, Y. Ma, Y. Ma, C.W. Glass, Z. Liu, T. Yu, O.O. Kurakevych, V.L. Solozhenko, Ionic high-pressure form of elemental boron. *Nature* **457** (2009) 863-867.

[20] A.R. Oganov, V.L. Solozhenko, Boron: a hunt for superhard polymorphs. *J. Superhard Mater.* **31** (2009) 285-291.

[21] P. Németh, L.A.J. Garvie, T. Aoki, N. Dubrovinskaia, L. Dubrovinsky, P.R. Buseck, Lonsdaleite is faulted and twinned cubic diamond and does not exist as a discrete material. *Nat. Commun.* **5** (2014) 5447.

[22] R. Hoffmann, A.A. Kabanov, A.A. Golov, D.M. Proserpio, Homo Citans and carbon allotropes: For an ethics of citation. *Angew. Chem. Int. Ed.* **55** (2016) 10962-10976; Samara Carbon Allotrope Database (http://sacada.sctms.ru)

[23] C.-X. Zhao, C.-Y. Niu, Z.-J. Qin, X.Y. Ren, J.-T. Wang, J.-H. Cho, Y. Jia, $H_{18}$ carbon: A new metallic phase with $sp^2$-$sp^3$ hybridized bonding network. *Sci. Rep.* **6** (2016) 21879.

[24] J. Tennyson, "Molecules in Space" in *Handbook of Molecular Physics and Quantum Chemistry*, Chichester: John Wiley & Sons, 2003, vol. 3, part III, p. 358.

[25] S.F. Matar, J. Etourneau, V.L. Solozhenko. First-principles investigations of tricarbon: From the isolated $C_3$ molecule to a novel ultra-hard anisotropic solid. *Carbon Trends* **6** (2021) 100132.

[26] W. Voigt, Über die Beziehung zwischen den beiden Elasticitätsconstanten isotroper Körper. *Annal. Phys.* **274** (1889) 573-587.

[27] V.A. Mukhanov, O.O. Kurakevych, V.L. Solozhenko, The interrelation between hardness and compressibility of substances and their structure and thermodynamic properties. *J. Superhard Mater.* **30** (2008) 368-378.

[28] A.O. Lyakhov, A.R. Oganov, Evolutionary search for superhard materials: Methodology and applications to forms of carbon and $TiO_2$. *Phys. Rev. B* **84** (2011) 092103.

[29] S.F. Matar, V.L. Solozhenko, Crystal chemistry and ab initio prediction of ultrahard rhombohedral $B_2N_2$ and $BC_2N$. *Solid State Sci.* **118** (2021) 106667.

[30] X. Yang,C. Lv, S. Liu, J. Zang. J. Qin, M. Du, D. Yang, X. Li, B. Liu, C.-X. Shan, Orthorhombic $C_{14}$ carbon: A novel superhard $sp^3$ carbon allotrope. *Carbon* **156** (2020) 309-312.

[31] Q. Fan, H. Liu, L. Jiang, X. Yu, W. Zhang, S. Yun, Two orthorhombic superhard carbon allotropes: $C_{16}$ and $C_{24}$. *Diam. Relat. Mater.* **116** (2021) 108426.

[32] Q. Fan, H. Liu, R. Yang, X. Yu, W. Zhang, S. Yun, An orthorhombic superhard carbon allotrope: *Pmma* $C_{24}$. *J. Solid State Chem.* **300** (2021) 122260.

[33] J. Chen, P. Ying, Y. Gao, X. Wei, B. Li, Q. Huan, K. Luo, Orthorhombic $C_{36}$: a $sp^2$–$sp^3$ carbon with pressure-induced metallization and superconductivity. *J. Mater. Sci.* **56** (2021) 17665-17673.

[34] V.L. Solozhenko, Y. Le Godec, A hunt for ultrahard materials. *J. Appl. Phys.* **126** (2019) 230401.

[35] Q. Wei, Q. Zhang, M.-G. Zhang, H.-Y. Yan, L.-X. Guo, B. Wei, A novel hybrid sp-$sp^2$ metallic carbon allotrope. *Front. Phys.* **13** (2018) 136105.

[36] S.F. Matar, V.L. Solozhenko, Novel ultrahard $sp^2/sp^3$ hybrid carbon allotrope from crystal chemistry and first principles: body-centered tetragonal $C_6$ ('neoglitter'). *ChemRxiv*. Cambridge: Cambridge Open Engage; 2022 (DOI: 10.26434/chemrxiv-2022-3d8pk)

[37] M.J. Bucknum, R. Hoffmann, A hypothetical dense 3,4-connected carbon net and related $B_2C$ and $CN_2$ nets built from 1,4-cyclohexadienoid units. *J. Am. Chem. Soc.* **116** (1994) 11456-11464.

[38] O.O. Kurakevych, V.L. Solozhenko, Rhombohedral boron subnitride, $B_{13}N_2$, by X-ray powder diffraction. *Acta Crystallogr. C* **63** (2007) i80-i82.

[39] V.L. Solozhenko, V. Bushlya, Mechanical properties of superhard boron subnitride $B_{13}N_2$. *J. Superhard Mater.* **39** (2017) 422-426.

[40] K.A. Cherednichenko, V.L. Solozhenko, Structure and equation of state of tetragonal boron subnitride $B_{50}N_2$. *J. Appl. Phys.* **122** (2017) 155901.

[41] V.L. Solozhenko, O.O. Kurakevych, Y. Le Godec, Creation of nanostuctures by extreme conditions: high-pressure synthesis of ultrahard nanocrystalline cubic boron nitride. *Adv. Mater.* **24** (2012) 1540-1544.

[42] V.L. Solozhenko, V. Bushlya, J. Zhou, Mechanical properties of ultra-hard nanocrystalline cubic boron nitride. *J. Appl. Phys.* **126** (2019) 075107.

[43] A.Y. Liu, M.L. Cohen, Prediction of new low compressibility solids. *Science* **245** (1989) 841-842.

[44] A.Y. Liu, R.M. Wentzcovitch, Stability of carbon nitride solids. *Phys. Rev. B* **50** (1994) 10362-10365.

[45] D. Teter, R.J. Hemley, Low-compressibility carbon nitrides. *Science* **271** (1996) 53-55.

[46] S.F. Matar, M. Mattesini, Ab initio search of carbon nitrides, isoelectronic with diamond, likely to lead to new ultra-hard materials. *C. R. Acad. Sci. Paris, Chimie* **4** (2001) 255-272.

[47] M. Mattesini, S.F. Matar, Density-functional theory investigation of hardness, stability, and electron-energy-loss spectra of carbon nitrides with $C_{11}N_4$ stoichiometry. *Phys. Rev. B* **65** (2002) 075110.

[48] E. Betranhandy, S.F. Matar, A model study for the breaking of cyanogen out of $CN_x$ within DFT. *Diam. Relat. Mater.* **15** (2006) 1609-1613.

[49] S.F. Matar, V.L. Solozhenko, The simplest dense carbon allotrope: Ultra-hard body-centered tetragonal $C_4$. *J. Solid State Chem.* **314** (2022) 123424.

[50] H. Werheit, A. Leithe-Jasper, T. Tanaka, H.W. Rotter, K.A. Schwetz, Some properties of single-crystal boron carbide. *J. Solid State Chem.* **177** (2004) 575-579.

[51] Y. Yao, J.S. Tse, D.D. Klug, Crystal and electronic structure of superhard $BC_5$: First-principles structural optimizations. *Phys. Rev. B* **80** (2009) 094106.

[52] H. Liu, Q. Li, L. Zhu, Y. Ma, Superhard polymorphs of diamond-like $BC_7$. *Solid State Comm.* **151** (2011) 716-719.

[53] S.F. Matar, Novel trigonal $BC_{11}$ as model structure of heavily doped diamond: Crystal chemistry rationale and first principles characterizations. *Diam. Relat. Mater.* **123** (2022) 108842.

[54] S.F. Matar, V.L. Solozhenko, Ultra-hard rhombohedral carbon by crystal chemistry and ab initio investigations. *J. Solid State Chem.* **302** (2021) 122354.

[55] Z. Liu, J. He, J. Yang, X. Guo, H. Sun, H.-T. Wang, E. Wu, Y. Tian, Prediction of a sandwichlike conducting superhard boron carbide: First-principles calculations. *Phys. Rev. B* **73** (2006) 172101.

[56] M. Mattesini, S.F. Matar, First-principles characterization of new ternary heterodiamond $BC_2N$ phases. *Comput. Mater. Sci.* **20** (2001) 107-119

[57] E. Kim, T. Pang, W. Utsumi, V.L. Solozhenko, Y. Zhao, Cubic phases of $BC_2N$: A first-principles study. *Phys. Rev. B* **75** (2007) 184115.

[58] X.F. Fan, H.Y. Wu, Z.X. Shen, J.-L. Kuo, A first-principle study on the structure, stability and hardness of cubic $BC_2N$. *Diam. Relat. Mater.* **18** (2009) 1278-1282.

[59] H. Wang, N. Qu, Q. Li, Y. Li, Z. Li, H. Gou, F. Gao, First-principles calculations on two superhard BCN allotropes: P-3m1-BCN and I41md-BCN. *Comput. Mater. Sci.* **184** (2020) 109869.

[60] X. Luo, X.-F. Zhou, Z. Liu, J. He, B. Xu, D. Yu, H.-T. Wang, Y. Tian, Refined crystal structure and mechanical properties of superhard $BC_4N$ crystal: First-principles calculations. *J. Phys. Chem. C* **112** (2008) 9516-9519.

[61] N.-R. Qu, H. Wang, Q. Li, Z.-P. Li, F.-M. Gao, An orthorhombic phase of superhard *o*-$BC_4N$. *Chin. Phys. Lett.* **36** (2019) 036201.

[62] L. Zhu, M. Ma, Q. Gao, B. Li, X. Wei, M. Xiong, Z. Zhao, J. He, Prediction of a series of superhard $BC_4N$ structures. *Diam. Relat. Mater.* **127** (2022) 109192

[63] X. Luo, X. Guo, Z. Liu, J. He, D. Yu, Y. Tian, H.-T. Wang, Ground-state properties and hardness of high density $BC_6N$ phases originating from diamond structure. *J. Appl. Phys.* **101** (2007) 083505.

[64] N.-R. Qu, H.-C. Wang, Q. Li, Y.-D. Li, Z.-P. Li, H.-Y. Gou, F.-M. Gao, Surperhard monoclinic $BC_6N$ allotropes: First-principles investigations. *Chin. Phys. B* **28** (2019) 096201.

[65] W.-C. Chen, J.N. Schmidt, D. Yan, Y.K. Vohra, C.-C. Chen, Machine learning and evolutionary prediction of superhard B-C-N compounds. *npj Comput. Mater.* **7** (2021) 114.

[66] F. Gao, J. He, E. Wu, S. Liu, D. Yu, D. Li, S. Zhang, Y. Tian, Hardness of covalent crystals. *Phys. Rev. Lett.* **91** (2003) 015502.

[67] S.F. Matar, V.L. Solozhenko, Novel superhard tetragonal BCN from crystal chemistry and first principles. *Materialia* **26** (2022) 101581.

[68] V.L. Solozhenko, V.V. Chernyshev, G.V. Fetisov, V.B. Rybakov, I.A. Petrusha, Structure analysis of the cubic boron nitride crystals. *J. Phys. Chem. Solids* **51** (1990) 1011-1012.

[69] E. Mazhnik, A.R. Oganov, Application of machine learning methods for predicting new superhard materials. *J. Appl. Phys.* **128** (2020) 075102.

[70] V.V. Brazhkin, V.L. Solozhenko, Myths about new ultrahard phases: Why materials that are significantly superior to diamond in elastic moduli and hardness are impossible. *J. Appl. Phys.* **125** (2019) 130901.

[71] P.D. Ownby, X. Yang, J. Liu, Calculated X-ray diffraction data for diamond polytypes. *J. Am. Ceram. Soc.* **75** (1992) 1876-1883.

[72] N. Bindzus, T. Straasø, N. Wahlberg, J. Becker, L. Bjerg, N. Lock, A.-C. Dippel, B.B. Iversen, Experimental determination of core electron deformation in diamond. *Acta Cryst. A* **70** (2014) 39-48.

[73] G.S. Manyali, R. Warmbier, A. Quandt, J.E. Lowther, Ab initio study of elastic properties of super hard and graphitic structures of $C_3N_4$. *Comput. Mater. Sci.* **69** (2013) 299-303.

## Annex: Computational framework

Accurate energy-based studies are primarily achieved within the framework of quantum mechanics. The most successful framework is the Density Functional Theory (DFT) whose theoretical basis was presented by Hohenberg and Kohn in 1964 [A1]. One year later, Kohn and Sham devised the so-called KS equations to efficiently solve the wave equation of the system [A2] using computational codes based on the DFT. Among the numerous programs, we used the plane-wave Vienna Ab initio Simulation Package (VASP) code [A3,A4] with the projector augmented wave (PAW) method [A4,A5] for the atomic potentials with all valence states, especially, in regard of light elements such as boron, carbon and nitrogen. The exchange-correlation effects inherent to DFT were considered with the generalized gradient approximation (GGA) following Perdew, Burke, and Ernzerhof (PBE) [A6]. PBE scheme was affirmed by Kilmes *et al*. as the best suited for quantum calculations of carbon structures [A7]. A conjugate-gradient algorithm [A8] was used in this computational scheme to relax the atoms onto the ground state. The tetrahedron method with Blöchl *et al*. corrections [A9] and Methfessel-Paxton scheme [A10] were applied for both geometry relaxation and total energy calculations, respectively. Brillouin-zone integrals were approximated using a special **k**-point sampling scheme by Monkhorst and Pack [A11]. The optimization of the structural parameters was performed until the forces on the atoms were less than 0.02 eV/Å, and all stress components below 0.003 eV/Å$^3$. The calculations were converged at an energy cut-off of 500 eV for the plane-wave basis set concerning the **k**-point integration in the Brillouin zone, with a starting mesh of 6×6×6 up to 12×12×12 for best convergence and relaxation to zero strains. In the post-treatment process of the ground state electronic structures, the electron localization function, the electronic and phonon band structures were computed, visualized and assessed. Calculations of phonon dispersion curves were also carried out to verify the dynamic stability of the proposed structures. The phonon modes were computed via finite displacements of the atoms off their equilibrium positions to obtain the forces from the summation over different configurations. The phonon dispersion curves along the direction of the Brillouin zone are subsequently obtained using "phonopy" code based on Python language [A12].

Further investigations of the electronic band structure and electron density of states were carried with the full-potential DFT-built augmented spherical wave ASW method [A13]. Fig. 4(c,d) shows the results of band structures calculations for template diamond-like *hex*-$C_{12}$ and resulting trigonal $BC_{11}$.

## Annex references


[A1] P. Hohenberg, W. Kohn, Inhomogeneous electron gas. *Phys. Rev. B* **136** (1964) 864-871.

[A2] W. Kohn, L.J. Sham, Self-consistent equations including exchange and correlation effects. *Phys. Rev. A* **140** (1965) 1133-1138.

[A3] G. Kresse, J. Furthmüller, Efficient iterative schemes for ab initio total-energy calculations using a plane-wave basis set. *Phys. Rev. B* **54** (1996) 11169.

[A4] G. Kresse, J. Joubert, From ultrasoft pseudopotentials to the projector augmented wave. *Phys. Rev. B* **59** (1999) 1758-1775.

[A5] P.E. Blöchl, Projector augmented wave method. *Phys. Rev. B* **50** (1994) 17953-17979.

[A6] J. Perdew, K. Burke, M. Ernzerhof, The Generalized Gradient Approximation made simple. *Phys. Rev. Lett.* **77** (1996) 3865-3868.

[A7] J. Klimeš, D.R. Bowler, A. Michaelides, Van der Waals density functionals applied to solids. *Phys. Rev. B* **83** (2011) 195131.

[A8] W.H. Press, B.P. Flannery, S.A. Teukolsky, W.T. Vetterling, *Numerical Recipes*, 2nd ed., Cambridge University Press: New York, USA, 1986.

[A9] P.E. Blöchl, O. Jepsen, O.K. Anderson, Improved tetrahedron method for Brillouin-zone integrations. *Phys. Rev. B* **49** (1994) 16223-16233.

[A10] M. Methfessel, A.T. Paxton, High-precision sampling for Brillouin-zone integration in metals. *Phys. Rev. B* **40** (1989) 3616-3621.

[A11] H.J. Monkhorst, J.D. Pack, Special k-points for Brillouin Zone integration. *Phys. Rev. B* **13** (1976) 5188-5192.

[A12] A. Togo, I. Tanaka, First principles phonon calculations in materials science. *Scr. Mater.* **108** (2015) 1-5.

[A13] V. Eyert, Basic notions and applications of the augmented spherical wave method. *Int. J. Quantum Chem.* **77** (2000) 1007-1031.

Table 1 (Ultra)hard phases of the B–C–N system: lattice parameters, density (ρ), Vickers hardness ($H_V$) and bulk moduli ($B_0$) calculated in the framework of thermodynamic model of hardness [27]

| | Space group | $a = b$ (Å) | $c$ (Å) | ρ (g/cm$^3$) | $H_V$ (GPa) | $B_0$ (GPa) |
|---|---|---|---|---|---|---|
| Diamond | *Fd*-3*m* | 3.56661 ‡ | | 3.517 | 98 *pw* | 445 § |
| Lonsdaleite | *P*6$_3$/*mmc* | 2.5221 † | 4.1186 † | 3.516 | 97 *pw* | 443 *pw* |
| *rh*-$C_3$ #166 [25] | *R*-3*m* | 2.4900 | 10.4100 | 3.211 | 89 | 406 |
| *hex*-$C_6$ #194 [25] | *P*6$_3$/*mmc* | 2.4950 | 6.9610 | 3.189 | 87 | 404 |
| *tet*-$C_6$ #119 [36] | *I*-4*m*2 | 2.4666 | 6.4320 | 3.058 | 85 | 385 |
| *c*-$C_3N_4$ #215 [44] | *P*-43*m* | 3.4300 | | 3.788 | 71 *pw* | 421 *pw* |
| *c*-$C_3N_4$ #220 [45] | *I*-43*d* | 5.3973 | | 3.889 | 73 *pw* | 430 *pw* |
| *tet*-$C_{11}N_4$ #115 [*pw*] | *P*-4*m*2 | 4.9526 | 3.5202 | 3.618 | 76 | 408 |
| *tet*-$BC_5$ #119 [51] | *I*-4*m*2 | 2.5250 | 11.3230 | 3.260 | 70 *pw* | 350 *pw* |
| *c*-$BC_7$ #215 [52] | *P*-43*m* | 3.6205 | | 3.320 | 72 *pw* | 358 *pw* |
| *trig*-$BC_{11}$ #156 [53] | *P*3*m*1 | 2.5381 | 12.5955 | 3.378 | 83 *pw* | 395 *pw* |
| *o*-$BC_2N$ #17 [56] | *P*222$_1$ | 3.5536/3.5986 | 3.5528 | 3.570 | 73 *pw* | 381 *pw* |
| *trig*-$BC_2N$ #156 [56] | *P*3*m*1 | 2.4955 | 4.1923 | 3.587 | 74 *pw* | 384 *pw* |
| *rh*-$BC_2N$ #160 [29] | *R*3*m* | 2.5382 | 12.6054 | 3.460 | 75 | 426 *pw* |
| *tet*-BCN #105 [67] | *P*4$_2$*mc* | 2.7047 | 6.0073 | 2.783 | 65 | 282 |

† Ref. 71

‡ Ref. 72

§ Ref. 70

*pw* present work

Table 2 Mechanical properties of (ultra)hard phases of the B–C–N system: Vickers hardness ($H_V$), bulk modulus ($B$), shear modulus ($G$), Young's modulus ($E$), Poisson's ratio (ν) and fracture toughness ($K_{Ic}$)

| | $H_V$ | | | | $B$ | | $G_V$ | $E$ [**] | ν [**] | $K_{Ic}$ [‡] |
|---|---|---|---|---|---|---|---|---|---|---|
| | T [*] | LO [†] | MO [‡] | CN [§] | $B_0$ [*] | $B_V$ | | | | |
| | GPa | | | | | | | | | MPa·m$^{1/2}$ |
| Diamond [*pw*] | 98 | 90 | 100 | 93 | 445 [††] | | 530 [††] | 1138 | 0.074 | 6.4 |
| Lonsdaleite [*pw*] | 97 | 90 | 99 | 94 | 443 | 432 | 521 | 1115 | 0.070 | 6.2 |
| *rh*-$C_3$ [#166] [25] | 89 | 83 | 73 [*pw*] | 65 [*pw*] | 406 | 394 | 402 | 900 | 0.119 | 5.1 |
| *hex*-$C_6$ [#194] [25] | 87 | 82 | 73 [*pw*] | 65 [*pw*] | 404 | 392 | 400 | 895 | 0.119 | 5.1 |
| *tet*-$C_6$ [#119] [36] | 85 | 78 | 68 [*pw*] | 63 | 385 | 366 | 375 | 839 | 0.118 | 4.7 |
| *c*-$C_3N_4$ [#215] [44] | 71 [*pw*] | 63 [*pw*] | 68 [*pw*] | 58 [*pw*] | 421 [*pw*] | 425 | 397 [***] | 908 [*pw*] | 0.144 [*pw*] | 7.1 [*pw*] |
| *c*-$C_3N_4$ [#220] [45] | 73 [*pw*] | 74 [*pw*] | 56 [*pw*] | 48 [*pw*] | 430 [*pw*] | 487 [§§] | 393 [§§] | 930 [§§] | 0.18 [§§] | 9.1 [*pw*] |
| *tet*-$C_{11}N_4$ [#115] [*pw*] | 76 | 78 | 87 | 82 | 408 | 406 | 461 | 1003 | 0.088 | 5.5 |
| *tet*-$BC_5$ [#119] [51] | 70 [*pw*] | 62 [*pw*] | 68 [*pw*] | 62 [*pw*] | 350 [*pw*] | 376 | 379 | 851 [*pw*] | 0.123 [*pw*] | 4.9 [*pw*] |
| *c*-$BC_7$ [#215] [52] | 72 [*pw*] | 59 [*pw*] | 75 [*pw*] | 70 [*pw*] | 358 [*pw*] | 375 | 403 | 890 [*pw*] | 0.104 [*pw*] | 4.8 [*pw*] |
| *trig*-$BC_{11}$ [#156] [53] | 83 [*pw*] | 81 [*pw*] | 75 [*pw*] | 68 | 395 [*pw*] | 405 | 414 | 926 [*pw*] | 0.119 [*pw*] | 5.3 [*pw*] |
| *o*-$BC_2N$ [#17] [56] | 73 [*pw*] | 69 [*pw*] | 88 [*pw*] | 76 [*pw*] | 381 [*pw*] | 459 | 482 | 1071 [*pw*] | 0.111 [*pw*] | 6.4 [*pw*] |
| *trig*-$BC_2N$ [#156] [56] | 74 [*pw*] | 58 [*pw*] | — | — | 384 [*pw*] | 420 | — | — | — | — |
| *rh*-$BC_2N$ [#160] [29] | 75 | 74 [*pw*] | 90 | 84 | 426 [*pw*] | 412 | 476 | 1031 | 0.083 | 5.7 |
| *tet*-BCN [#105] [67] | 65 | 61 | 35 [*pw*] | 36 | 282 | 280 | 232 | 545 | 0.175 | 4.2 |

[*] Thermodynamic model [27]

[†] Lyakhov-Oganov model [28]

[‡] Mazhnik-Oganov model [10]

[§] Chen-Niu model [8]

[**] $E$ and ν values calculated using isotropic approximation

[††] Ref. 70

[***] Calculated from elastic moduli $C_{ij}$ [44] using Voigt's approach [26]

[§§] Ref. 73

[*pw*] present work

Table 3 Vickers hardness of hypothetical ternary B–C–N phases calculated using different models.

| | $H_V$ (GPa) | | |
|---|---|---|---|
| | Gao's model [*] | Tian's model [†] | Thermodynamic model [‡] |
| *c*-$BC_2N$ [58] | 79.7 | — | 75 [pw] |
| *trig*-$BC_4N$ (*P*3*m*1) [60] | 84.3 | — | 76 [pw] |
| *o*-$BC_4N$ (*Imm*2) [61] | 78.7 | — | 73 [pw] |
| *trig*-$BC_4N$ [62] | — | 87.5 | 73 [pw] |
| *tet*-$BC_6N$ (*P*−42*m*) [63] | 79.9 | — | 75 [pw] |
| *rh*-$BC_6N$ (*R*3*m*) [63] | 79.1 | — | 76 [pw] |
| *m*-$BC_6N$ (*Pm*) [64] | 77.4 | — | 72 [pw] |
| *m*-$BC_6N$ (*Cm*) [64] | 80.6 | — | 73 [pw] |
| *trig*-$BC_{10}N$ (*P*3*m*1) [65] | — | 87 | 75 [pw] |
| *tet*-BCN ($I4_1md$) [59] | 61.8 | — | 70 [pw] |
| *trig*-BCN (*P*-3*m*1) [59] | 68.5 | — | 69 [pw] |

[*] Ref. 66

[†] Ref. 9

[‡] Ref. 27

[pw] present work

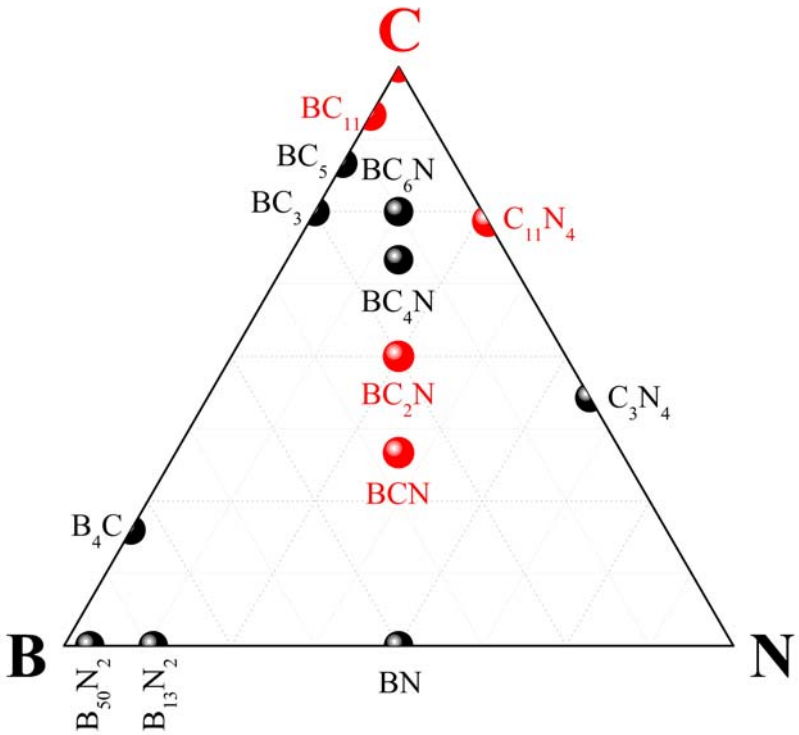


Fig. 1 Superhard phases of the B–C–N ternary system. Ultrahard phases discussed in the present paper are shown in red.

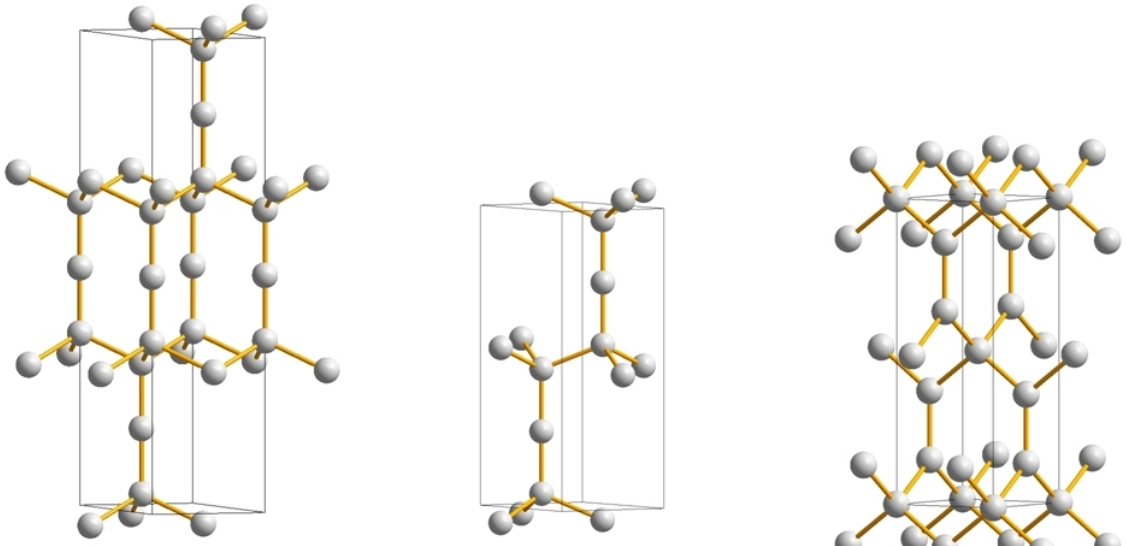

(*a*) (*b*) (*c*)

Fig. 2 Novel ultrahard carbon allotropes: 'tricarbons' – rhombohedral $C_3$ (*a*) and hexagonal $C_6$ (*b*) (both structures are in hexagonal setting); and tetragonal $C_6$ 'neoglitter' (*c*).

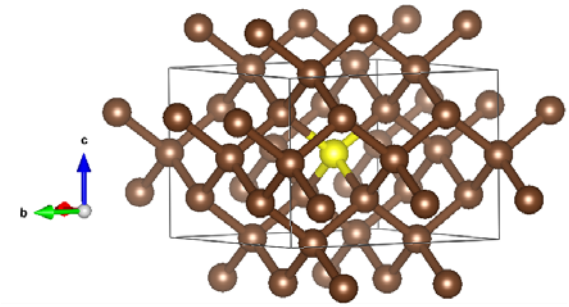

(*a*)

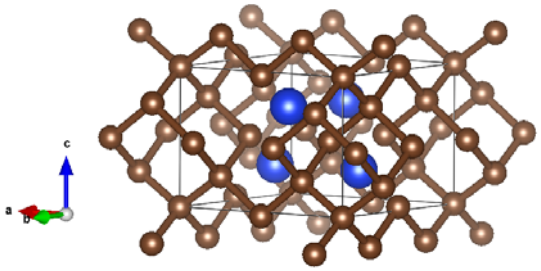

(*b*)

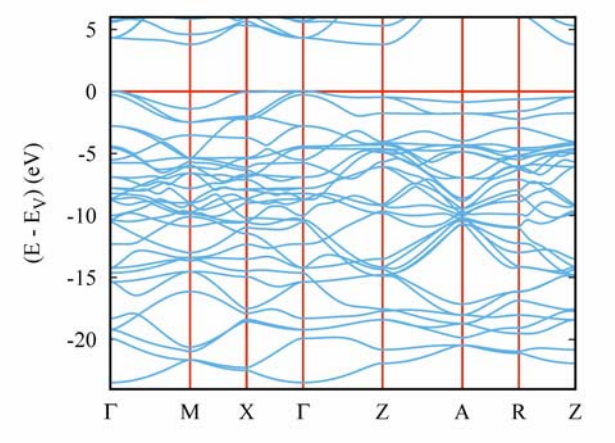


(*c*)

Fig. 3 Novel ultrahard carbon subnitride: crystal structures of template diamond-like $C_{16}$ (*a*) and tetragonal $C_{11}N_4$ (*b*); electronic band structure of $C_{11}N_4$ (*c*).

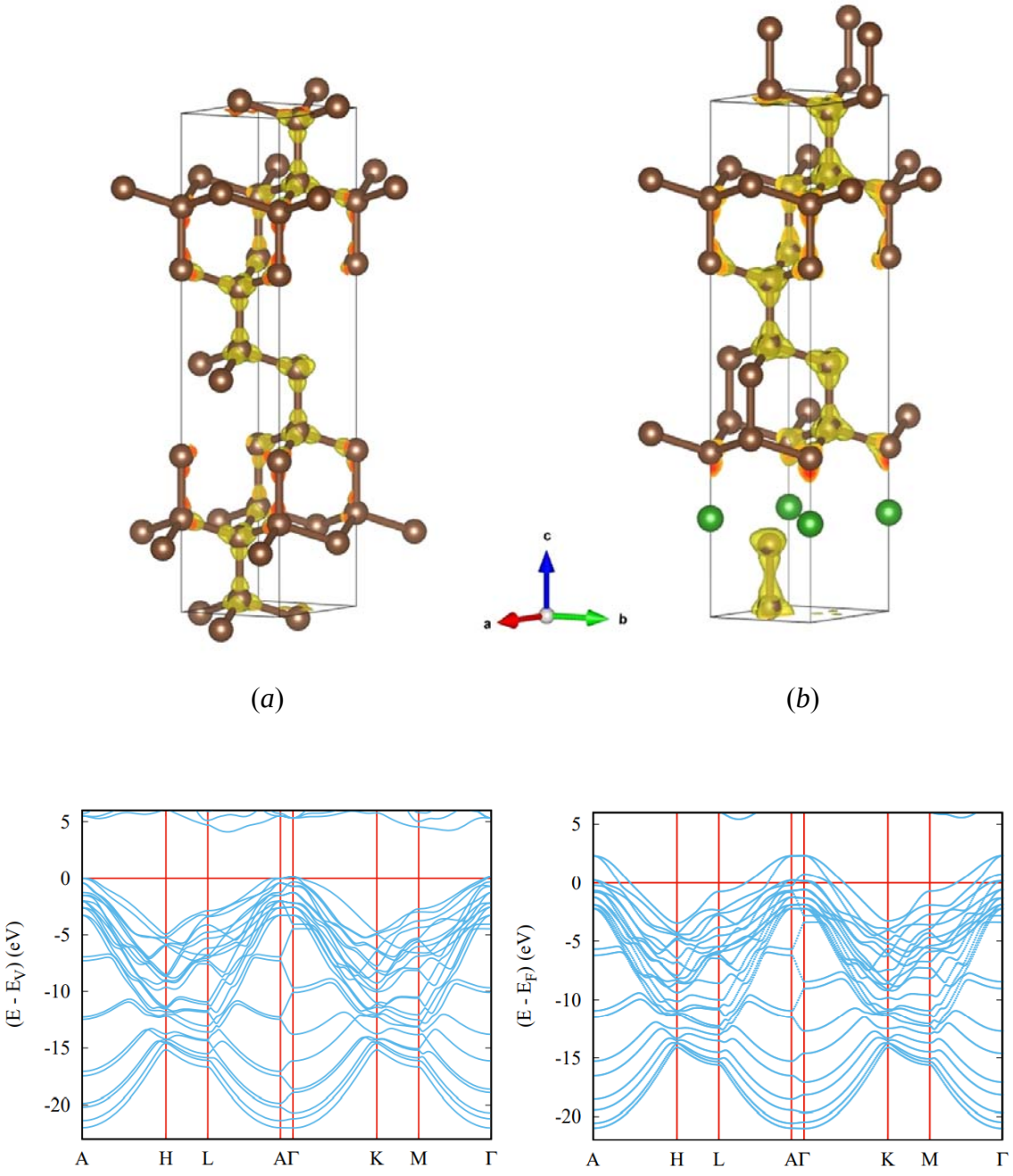


Fig. 4 Ultrahard carbon-rich boron carbide: crystal structures of template hexagonal $C_{12}$ (*a*) and trigonal $BC_{11}$ (*b*) with charge density distributions, and electronic band structures of insulating *hex*-$C_{12}$ (*c*) and metallic $BC_{11}$ (*d*). Boron atoms are shown by green spheres.

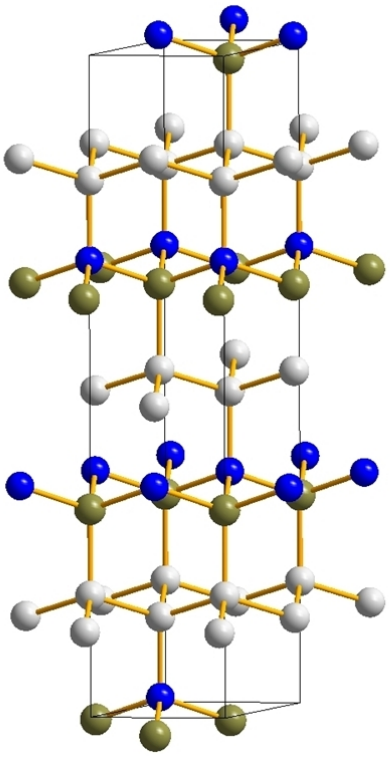

(*a*)

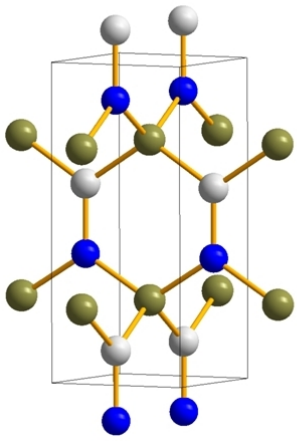

(*b*)

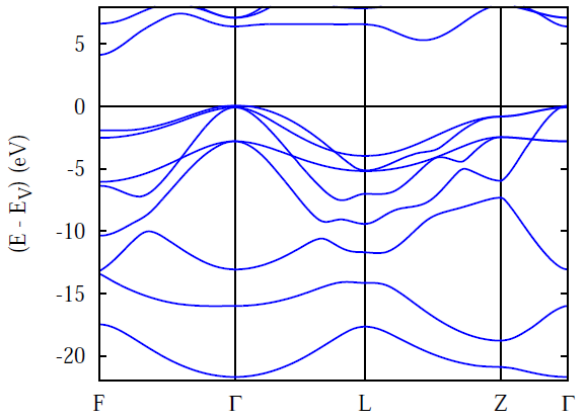


(*c*)

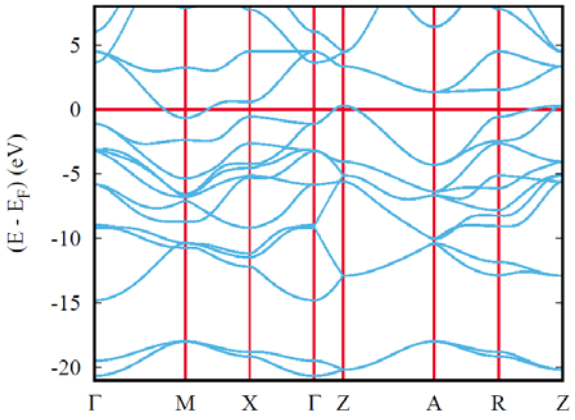


(*d*)

Fig. 5 Crystal structures (*a, b*) and electronic band structures (*c, d*) of rhombohedral $BC_2N$ and tetragonal BCN. Boron, carbon and nitrogen atoms are shown by olive, white and blue spheres, respectively.

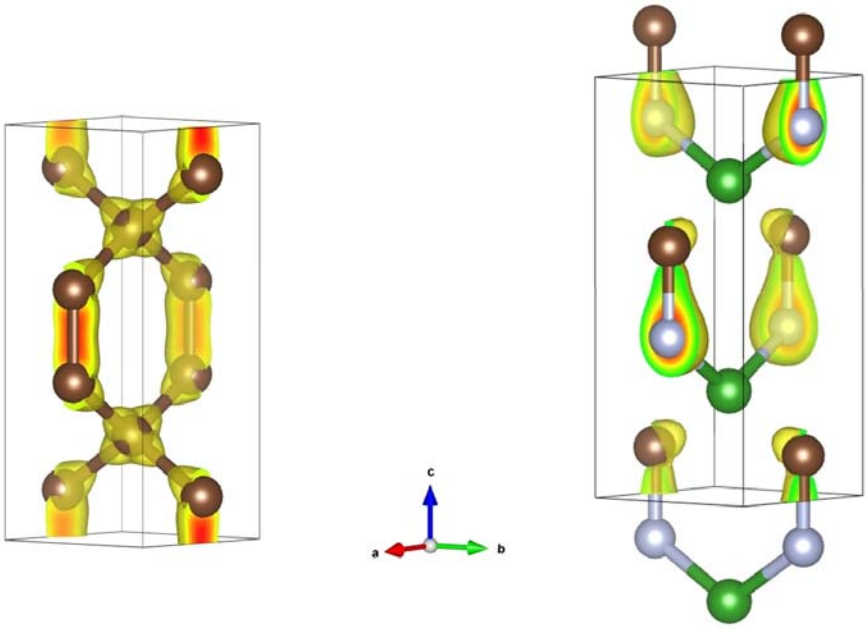


(*a*) (*b*)

Fig. 6 Crystal structures of template 'glitter' $C_6$ (*a*) and tetragonal BCN (*b*) with charge density distributions. Boron, carbon and nitrogen atoms are shown by green, brown and grey spheres, respectively.